Aalto University
School of Chemical
Engineering

MICROBIOTA-DRIVEN α-SYNUCLEIN PATHOLOGY IN THE GUT: A HISTOLOGICAL AND MOLECULAR STUDY

Lauri Tossavainen

Master´s Programme in Life Science Technology

Major in Biosystems Engineering

Master’s thesis for the degree of Master of Science in Technology submitted for inspection, Espoo, 09 Month, 2025.

Supervisor Professor Paula Jouhten

Instructors Merja Voutilainen, Shibajee Mandal

Author Lauri Tossavainen

Title of thesis Microbiota-Driven α-Synuclein Pathology in the Gut: A Histological and Molecular Study

Degree Programme Life Sciences Technology

Major Biosystems and Biomaterials Engineering

Thesis supervisor Paula Jouhten

Thesis advisor(s) / Thesis examiner(s) Merja Voutilainen

Date 29.09.2025 **Number of pages** 36 **Language** English

Abstract

Parkinson's disease (PD) is the second most common neurodegenerative disorder, yet its causes remain incompletely understood. In addition to genetic and cellular factors, the gut microbiome has been proposed to play a role in disease initiation and progression. Among intestinal microbes, sulfate-reducing *Desulfovibrio* (DSV) species such as DSV *desulfuricans* have been suggested to promote aggregation of alpha-synuclein, a hallmark of Parkinson's diseas pathology, and colonization with human-derived isolates has been shown to induce PD relevant features in *Caenorhabditis elegans*. These observations raise the question of whether *D. desulfuricans* can similarly drive pathological changes in mammalian hosts.

This thesis investigated whether colonization with *D. desulfuricans* strains influences colonic pathology in wild-type mice. Animals were randomly assigned to experimental and control groups and received bacterial suspensions by oral gavage three times weekly for four weeks. Distal colons were collected and processed for histological analysis, including staining for phosphorylated alpha-synuclein, enteroendocrine cells (EEC) using Chromogranin A (CgA), goblet cells, and immune cell infiltration. Digital imaging and quantitative analysis were applied to evaluate pathological markers. The analyses revealed no significant differences between groups in alpha-synuclein aggregate numbers, EEC counts, EEC–aggregate proximity, goblet cell distribution, or immune infiltration. Only a small fraction of alpha-synuclein aggregates localized within 10 micrometers of the nearest EEC, suggesting limited direct spatial association under these conditions.

These findings indicate that short-term colonization with *D. desulfuricans* is not sufficient to induce PD-like pathology in the mouse colon. Although the results do not support a direct and immediate role for *D. desulfuricans* in triggering gut pathology, they provide a baseline for refining microbial models of PD. Future studies incorporating longer treatment periods, genetically susceptible mouse strains, or community-level microbial interactions are needed to determine whether gut microbes act as modulators or initiators of PD related pathology.

Keywords Parkinson's Disease, Microbiome, *Desulfovibrio Desulfuricans,* alpha-synuclein, enteroendocrine cells, Inflammation, Mouse model

Tekijä Lauri Tossavainen

Työn nimi Mikrobiomin ohjaama α-synukleiinipatologia suolistossa: Histologinen ja molekulaarinen tutkimus

Koulutusohjelma Life Science Technology

Pääaine Biosystems and Biomaterials Engineering

Työn valvoja Paula Jouhten

Työn ohjaaja(t)/Työn tarkastaja(t) Merja Voutilainen

Päivämäärä 29.09.2025 **Sivumäärä** 36 **Kieli** Suomi

Tiivistelmä

Parkinsonin tauti on toiseksi yleisin neurodegeneratiivinen sairaus, mutta sen taustalla olevia syitä ei vielä täysin tunneta. Geneettisten ja solutason tekijöiden lisäksi suolistomikrobiomin on ehdotettu vaikuttavan taudin puhkeamiseen ja etenemiseen. Suolistomikrobeista erityisesti sulfaattia pelkistävien *Desulfovibrio*-bakteerien, kuten *Desulfovibrio desulfuricans* -lajin, on esitetty edistävän α-synukleiinin aggregaatiota, joka on keskeinen Parkinsonin taudin patologinen tunnusmerkki. Ihmisperäisillä kannoilla on osoitettu olevan Parkinsonin tautiin liittyviä vaikutuksia *Caenorhabditis elegans* -mallissa. Tämä herättää kysymyksen, voiko *D. desulfuricans* aiheuttaa samankaltaisia patologisia muutoksia myös nisäkkäillä.

Tässä työssä tutkittiin, vaikuttaako *D. desulfuricans* -kantojen kolonisaatio villityyppisten hiirten paksusuolen patologiaan. Eläimet jaettiin satunnaisesti koe- ja kontrolliryhmiin, ja niille annettiin bakteerisuspensioita suun kautta kolme kertaa viikossa neljän viikon ajan. Hiirten distaaliset paksusuoliosat kerättiin ja analysoitiin histologisesti fosforyloidun α-synukleiinin, enteroendokriinisten solujen, pikarisolujen ja immuunisolujen infiltraation osalta. Digitaalinen kuvantaminen ja kvantitatiivinen analyysi toteutettiin patologisten merkkien arvioimiseksi.

Tulokset osoittivat, ettei ryhmien välillä ollut merkittäviä eroja α-synukleiiniaggregaatioiden määrässä, enteroendokriinisten solujen määrässä, näiden solujen ja aggregaattien välisessä etäisyydessä, pikarisolujen jakaumassa tai immuunisolujen infiltraatiossa. Vain pieni osa α-synukleiiniaggregaateista paikantui alle 10 mikrometrin etäisyydelle enteroendokriinisoluista, mikä viittaa vähäiseen suoraan yhteyteen näissä olosuhteissa.

Havainnot viittaavat siihen, että lyhytaikainen *D. desulfuricans* -kolonisaatio ei riitä aiheuttamaan Parkinsonin tautiin liittyvää patologiaa hiiren paksusuolessa. Vaikka tulokset eivät tue suoraa ja välitöntä roolia *D. desulfuricans* -lajin toiminnassa suolistopatologian käynnistäjänä, ne tarjoavat lähtökohdan Parkinsonin taudin mikrobimallien jatkokehitykselle. Tulevissa tutkimuksissa pidemmät hoitojaksot, geneettisesti alttiit hiirikannat sekä mikrobiyhteisöjen vuorovaikutusten tarkastelu voivat olla tarpeen, jotta suolistomikrobien merkitys Parkinsonin taudin modulaattoreina tai käynnistäjinä voidaan selvittää.

Avainsanat: Parkinsonin tauti, Mikrobiomi, *Desulfovibrio desulfuricans*, alpha-synukleiini, Enteroendokriinisolu, Tulehdus, Hiirimalli

Preface and Acknowledgements

I would like to offer my thanks firstly to my primary advisor Merja Voutilainen, as well as my unofficial advisor Khosrow Mohammadi at Helsinki University for the opportunity to do my master’s thesis in an interesting topic and supportive environment. Without their assistance in matters of knowledge and procedure, I could’ve never carried out all the experiments needed for this thesis. Furthermore, my colleagues at the Regenerative Neuroscience lab also have my eternal gratitude for their day-to-day assistance in allowing me to learn from them, counseling on protocol optimization, discussions on the relevant wider scientific contexts, as well as helping me maintain my sanity during this process. Specifically, I would like to offer special thanks to Aastha Singh, and Stanislav Rozov. The former was a true lifeline for their diligent help learning all of my staining protocols and ordering me to get some sleep every once in a while. The ladder for their seemingly infinite knowledge base, applied to any question that arose throughout the experiments and procedures carried out throughout this process.

Furthermore, the facilities and expertise of the BI Histology core facility at the University of Helsinki, supported by HiLIFE, are gratefully acknowledged. Part of the work was carried out with the support of HiLIFE Laboratory Animal Centre Core Facility, University of Helsinki, Finland. I am grateful for their assistance in learning how to carry out the necessary procedures on mice.

Finally, I would like to thank my thesis supervisor Paula Jouhten for her assistance and guidance in this process. Her help was invaluable in the writing stage of this thesis

Table of contents

List of symbols and abbreviations

PD – Parkinson’s disease

ENS – Enteric nervous system

CNS – Central nervous system

EEC – Enteroendocrine cell

DSV – Desulfovibrio

CFU – Colony-forming unit

PBS – Phosphate-buffered saline

PRAS – Pre-reduced anaerobic phosphate-buffered saline

PFA – Paraformaldehyde

ROI – Region of interest

IHC – Immunohistochemistry

TBS-T – TBS + Tween 20 solution

ABC – Avidin–biotin complex

DAB – 3,3’-Diaminobenzidine

SEM – Standard error of the mean

FMT – Fecal microbiota transplantati

1 Introduction

Although PD is defined pathologically by the loss of dopaminergic neurons in the substantia nigra and the accumulation of α-synuclein aggregates (Kalia & Lang, 2015), its clinical and biological presentation is highly heterogeneous. Increasing evidence points to early pathological events outside the brain, particularly in the gastrointestinal tract, prompting the proposal that PD may in some cases originate in the gut (Braak et al., 2003; Borghammer & Van Den Berge, 2019). This gut–brain axis hypothesis is supported by findings of α-synuclein inclusions in intestinal biopsies years before motor onset (Shannon et al., 2012) and by experimental studies demonstrating retrograde propagation of pathology along the vagus nerve (Kim et al., 2019).

Epidemiological evidence also supports the gut–brain axis hypothesis, as several large cohort studies have reported a reduced risk of PD following truncal vagotomy (Svensson et al., 2015). Nevertheless, it is increasingly recognized that PD is a heterogeneous disorder with multiple possible sites of pathological initiation. The gut-first model does not account for all cases, and a brain-first subtype has been described in which α-synuclein aggregation originates in central regions such as the amygdala or olfactory bulb before extending peripherally (Borghammer & Van Den Berge, 2019).

Within this broader context of heterogeneity, attention has shifted to environmental factors that could act as triggers or modifiers of disease. Among the various environmental and microbial influences proposed to contribute to PD, the intestinal microbiota has emerged as a key factor of interest. Altered microbial composition in PD patients has been reported in several studies (Romano et al., 2021; Lubomski et al., 2022), and fecal microbiota transplantation (FMT) experiments suggest that these microbial shifts can influence both motor function and α-synuclein pathology in animal models (Yang et al., 2024). Yet, the specific microbial drivers and their mechanisms of action remain elusive.

One group of microbes has drawn particular attention. Recent attention has focused on sulfate-reducing bacteria of the genus *Desulfovibrio* (DSV). These microbes are consistently enriched in the gut microbiota of PD patients compared to healthy controls (Murros et al., 2021; Bedarf et al., 2017) and are known to produce hydrogen sulfide, which at elevated concentrations can inhibit cytochrome c oxidase and impair mitochondrial respiration (Carbonero et al., 2012). Importantly, DSV strains isolated from PD patients have been shown to promote α-synuclein aggregation in model organisms such as Caenorhabditis elegans (Huynh et al., 2023). Despite these findings, it remains unclear whether colonization with human-derived DSV strains can induce histopathological changes in mammalian hosts, or whether isolates from PD patients differ in pathogenic potential from those carried by healthy individuals.

This gap in knowledge provides the rationale for the present study. This study addresses these questions by investigating the impact of PD patient derived and healthy-donor derived DSV strains on gut pathology in wild-type mice. Using a combination of microbial colonization, immunohistochemistry (IHC), and molecular methods, the study evaluates whether these bacteria disrupt colonic tissue architecture, promote α-synuclein aggregation, and contribute to features of gut–brain axis pathology.

The aim of this work is to clarify the potential role of DSV in initiating or modulating PD-related pathology. The central hypothesis is that colonization with PD-derived DSV strains promotes α-synuclein aggregation and colonic dysfunction to a greater extent than strains derived from healthy controls. By integrating microbial, histological, and molecular analyses, this study seeks to provide novel evidence on how specific gut bacteria may contribute to the pathogenesis of PD, thereby informing broader models of disease heterogeneity and gut–brain interactions.

2 Literature review

PD is a multifactorial neurodegenerative disorder with both motor and non-motor symptoms, whose pathogenesis continues to be a subject of intense research and debate (Jenner et al., 2013). While PD classically presents with tremors, rigidity, and bradykinesia, its non-motor features such as anosmia, sleep disturbances, and gastrointestinal dysfunction often precede diagnosis by years or even decades (Kouli et al., 2018; Kalia & Lang, 2015). This has led to the rise of the gut-first hypothesis, which posits that PD pathology may originate in the enteric nervous system (ENS) and spread to the brain via the vagus nerve (Kim et al., 2019; Borghammer & Van Den Berge, 2019). Braak's staging framework identified the dorsal motor nucleus of the vagus and the anterior olfactory structures as earliest sites of Lewy pathology (Braak et al., 2003; Braak & Del Tredici, 2017). This pattern was later further developed into the dual-hit hypothesis, proposing that environmental agents might initiate α-synuclein pathology via both the gut–vagus and olfactory routes (Hawkes et al., 2007). It should be kept in mind that this gut-focused model is just one among several competing frameworks. Comprehensive reviews have suggested that the pathogenesis of PD is highly heterogeneous, with proposed mechanisms encompassing gut-origin pathways, brain-first processes, genetic susceptibilities, mitochondrial dysfunction, and exposure to environmental toxins (Nuzum et al., 2022; Johnson et al., 2022).

2.1 The Gut-brain axis theory

The gut-brain axis hypothesis gained traction from the observation that α-synuclein aggregates, which are considered hallmarks of PD pathology, were found in the gastrointestinal tract years before motor symptoms arise. Kouli et al. (2018) noted early involvement of both the dorsal motor nucleus and enteric plexuses, consistent with Braak's staging and later dual-hit interpretations (Hawkes et al., 2007). Indeed, experiments where α-synuclein fibrils were injected into the intestinal wall of rodents have shown retrograde transport and aggregation in the brainstem, reinforcing the concept of prion-like spread (Kim et al., 2019).

An additional line of evidence supporting the gut-first model has focused on EECs as potential initiators of α-synuclein pathology. EECs are specialized epithelial cells that act as sensory transducers, releasing hormones and neurotransmitters in response to luminal stimuli and forming direct synapse-like connections with enteric nerves (Bohórquez et al., 2015). Importantly, α-synuclein expression has been demonstrated in subsets of EECs within the intestinal mucosa (Hilton et al., 2014). This observation has led to the hypothesis that EECs may serve as the initial site of α-synuclein misfolding, driven by exposure to dietary, microbial, or inflammatory stressors. Through their neuroepithelial connections, misfolded α-synuclein could then propagate from EECs into the ENS, and subsequently to the central nervous system (CNS) via prion-like transmission along the vagus nerve (Chandra et al., 2017). Such a mechanism would position EECs as a cellular interface between environmental triggers in the gut lumen and the neuronal pathways implicated in PD progression, making them a compelling target for further mechanistic studies.

Moreover, the microbiome's role in modulating risk for PD has received increasing attention. Sampson et al. (2016) demonstrated that transplanting gut microbiota from PD patients into mice exacerbated motor symptoms and α-synuclein pathology. Such findings suggest that microbial composition influences neuroinflammatory and α-synuclein aggregation processes. However, the exact microbial culprits and mechanisms remain debated, and causality has not been studied.

2.2 Specific microbial candidates: Desulfovibrio

Among candidate taxa implicated in PD, sulfate-reducing bacteria of the genus Desulfovibrio (DSV) have gained attention in recent years (Murros et al., 2021; Huynh et al., 2023). Sulfate-reducing bacteria produce hydrogen sulfide, which is toxic to colonocytes in excess, notably by impairing butyrate oxidation and contributing to mucosal inflammation (Carbonero et al., 2012). Notably, DSV strains isolated from PD patients have been shown to promote α-synuclein aggregation in C. elegans (Huynh et al., 2023). It is important to note that C. elegans is typically maintained on a simplified near-monoculture bacterial diet, classically Escherichia coli OP50, which may amplify strain-level microbial effects compared to more complex mammalian systems (Stiernagle, 2006). Epidemiological studies have consistently shown that the fecal microbiota of PD patients differs significantly from that of healthy controls, with reductions in butyrate-producing genera and enrichment of potentially proinflammatory taxa (Keshavarzian et al., 2015; Gerhardt & Mohajeri, 2018). However, whether such microbial shifts play a causal role in disease initiation, or whether they reflect secondary changes in the gut environment, remains an open question. This raises the need to explore mechanistic links, including microbial toxins, barrier disruption, and inflammation.

2.3 Mechanistic gaps: inflammation, toxins, and aggregation

The precise mechanisms by which gut microbes influence α-synuclein pathology remain poorly defined. Hypotheses include microbial metabolites acting as toxins, disruption of the intestinal epithelial barrier, or induction of chronic low-grade inflammation (Sampson et al., 2016; Houser & Tansey, 2017). Desulfovibrio species are of particular interest because of their ability to generate H_2S, which could impair host mitochondrial function and immune signaling (Carbonero et al., 2012; Huynh et al., 2023). These stressors may accelerate α-synuclein misfolding within enteric neurons, initiating pathology that can propagate to the brain via prion-like mechanisms. Despite these plausible pathways, experimental validation in mammalian systems has remained scarce, and most current evidence has derived from invertebrate models or correlative human studies (Huynh et al., 2023; Sampson et al., 2016). This study therefore addresses a critical mechanistic gap by directly testing whether colonization with human-derived DSV strains can trigger histological and molecular signatures of PD pathology in mice.

2.4 Gut histology as a readout

While studies focusing on the CNS dominate PD research (Kalia & Lang, 2015), gut histology provides an equally important method to study early disease processes. Goblet cells, which secrete mucins forming the intestinal barrier, are often depleted in conditions of dysbiosis and chronic inflammation (Pelaseyed et al., 2014b). Reduced mucus integrity can allow microbial products to interact more directly with the ENS, potentially accelerating α-synuclein aggregation. Histological features such as crypt architecture and immune cell infiltration are additional markers of epithelial stress and inflammatory activation (Pelaseyed et al., 2014a). Yet, relatively few PD–microbiome studies include detailed colonic histology alongside molecular endpoints, leaving unanswered whether microbial perturbations translate into measurable barrier dysfunction. By integrating Alcian Blue and IHC staining, the present study examined whether DSV colonization alters these structural features in ways that could facilitate ENS-CNS pathology.

2.5 Integrated microbial, histological, and molecular approaches

Methodological limitations also hinder synthesis across the PD–microbiome field. Studies based solely on sequencing can identify associations between microbes and disease, but they rarely establish causality or demonstrate downstream histopathology. Conversely, CNS models employing viral α-syn overexpression or fibril injections provide mechanistic insights into aggregation and propagation but have neglected the role of microbial triggers (Luk et al., 2012; Rey et al., 2013). Integrated approaches that combine microbial colonization with histological and molecular analyses are therefore essential. Previous FMT studies confirmed that PD-derived microbial communities can worsen motor dysfunction, though such designs cannot isolate the role of individual taxa (Sampson et al., 2016). By narrowing the focus to human-derived *Desulfovibrio* strains, and linking colonization with both gut and brain pathology, this study advanced a more causally informative model. The integrated pipeline allowed for a system-level assessment of how specific microbes may interface with both the intestinal barrier and neurodegenerative processes.

Considering the topic critically, not all PD cases fit the gut-first model. Borghammer and Van Den Berge (2019) introduced a brain-first subtype, proposing that for a subset of patients, α-synuclein pathology begins in the amygdala or olfactory bulb and later affects the periphery. Autopsy data also show that enteric α-synuclein pathology is not universal in PD. For instance, Beach et al. (2010) found phosphorylated α-synuclein in stomach tissue in 81% and in the vagus nerve in 89% of PD cases, implying a subset without detectable ENS involvement, which demonstrated that α-synuclein pathology can be absent in the ENS in a subset of PD cases. Furthermore, Kouli et al. (2018) described how Lewy pathology is inconsistently distributed and that some patients deviate from the Braak staging model altogether. Thus, the gut-brain axis may only account for a subset of cases.

Thus, a broader etiological framework for PD should incorporate genetic susceptibility, environmental exposures, and systemic dysfunction. Kouli et al. (2008) identify over 20 PARK genes linked to familial or risk-modifying PD. Mutations in LRRK2, GBA, PINK1, and SNCA influence mitochondrial quality control, lysosomal function, and protein degradation, aligning with pathophysiological processes like impaired mitophagy and α-synuclein misfolding. Environmental risk factors, such as pesticide exposure, rural living, and heavy metal exposure, have also been associated with an increased PD incidence. On the other hand, smoking and caffeine consumption appear protective, although mechanisms are unclear and confounded by reverse causality hypotheses (Kouli et al., 2018).

Methodological diversity complicates synthesis across studies, with experimental models ranging from molecular to epidemiological scales. While some use in vivo rodent or worm models, such as pre-formed fibril injections into the brain to seed endogenous α-synuclein aggregation (Luk et al., 2012), or viral overexpression of human α-synuclein in peripheral nerves to track propagation (Rey et al., 2013), others rely on patient-derived microbiota or epidemiological datasets (Sampson et al., 2016; Gao et al., 2011)., others rely on patient-derived microbiota or epidemiological datasets (Sampson et al., 2016; Gao et al., 2011). Each approach provides insights, but limitations in translation, sample variability, and control of confounders hinder consensus (Johnson et al., 2019; Nuzum et al., 2022). For example, Burke et al. (2008) highlighted that Braak staging does not consistently correlate with clinical severity and fails to account for patients who never follow the proposed caudo–rostral progression, raising doubts about its universality. More recently, Andersen et al. (2025) emphasized additional methodological challenges of cross-sectional autopsy designs, including limited sample sizes and difficulties inferring temporal order. Conversely, prospective cohort studies, such as those examining prodromal symptoms or environmental exposures, face problems of retrospective bias and variable diagnostic thresholds (Zhang et al., 2024).

In conclusion, while the gut-brain axis hypothesis offers an appealing framework for early intervention and explains several prodromal features of PD, it is not universally applicable. The multifactorial etiology of PD that spans genetics, environment, and systemic vulnerability suggests that the disease may emerge through multiple parallel or converging pathways. Future work must refine subtype definitions, embrace longitudinal multi-modal studies, and explore biomarkers that can distinguish gut-first from brain-first progression. Only then can research methodologies and therapeutic strategies be tailored to the complex biology underlying this heterogeneous disorder. The gut-brain axis provides an attractive and testable model for early detection and intervention in some PD subtypes, but it does not universally account for all observed clinical and pathological features. A stratified approach acknowledging both gut-first and brain-first pathways may help reconcile conflicting findings and better tailor therapeutic strategies.

3 Materials and Methods

3.1 Animals and Treatment Groups

A total of 50 male wild-type mice, aged 20 weeks and weighing 28–34 g at the start, were used. Animals were housed in groups of 1–5 per cage under controlled environmental conditions (12:12 h light–dark cycle, 22 °C ambient temperature, 50–60% relative humidity) with ad libitum access to food and water. Each mouse was assigned an individual identification number and randomly allocated into four groups matched by body weight: negative control (n = 5), positive control (*E. coli K-12*; n = 15), *D. desulfuricans* isolate from a PD patient (DSV-PD; n = 15), and *D. desulfuricans* isolate from a healthy donor (DSV-Healthy; n = 15).

3.2 Preparation of positive control and treatment group suspensions

3.2.1 Culturing of *E. coli* K-12 in LB Broth

The laboratory strain Escherichia coli K-12 was cultured aerobically using the DSMZ-recommended Luria–Bertani (LB) medium (DSMZ Medium 381). The medium composition per liter consisted of 10 g tryptone, 5 g yeast extract, and 10 g NaCl, dissolved in distilled water, and the pH was adjusted to 7.0 prior to sterilization. For solid medium, 20 g/L agar was added. All media were sterilized by autoclaving at 121 °C for 20 min.

Cultures were initiated from glycerol stocks stored at –80 °C. Stocks were first streaked on LB agar plates and incubated overnight at 37 °C to obtain single colonies. Individual colonies were then used to inoculate liquid precultures, prepared in Erlenmeyer flasks containing 50 mL of LB medium in 250 mL vessels, and grown overnight at 37 °C with agitation at 180 rpm to ensure adequate aeration.

For experimental cultures, overnight precultures were diluted 1:100 into fresh LB medium and grown under identical conditions. Cultures were monitored spectrophotometrically until they reached the exponential growth phase, at which point they were prepared for downstream processing. Growth in the mid-logarithmic phase was selected to ensure high cell viability and reproducibility across batches.

3.2.2 Culturing of human-isolated D. desulfuricans

Human-derived strains of *D. desulfuricans* were cultured under strict anaerobic conditions in DSMZ Medium 641 (MV Medium), following DSMZ specifications. The basal medium was sparged with nitrogen gas to displace oxygen before autoclaving at 121 °C for 20 min. After cooling, sterile-filtered solutions of sodium lactate (60 mM), sodium sulfide nonahydrate (1 mM), sodium bicarbonate (30 mM), and vitamin and trace element mixes were added aseptically. Resazurin (1 mg/L) was included as a redox indicator, and the pH was adjusted to 7.0–7.2.

Inocula were prepared from frozen glycerol stocks, which were transferred into Hungate tubes or sealed serum bottles containing 10–50 mL of MV medium. All manipulations were carried out inside an anaerobic chamber (N_2/H_2/CO_2, 80:10:10) to prevent oxygen exposure. When required, sodium dithionite (10–20 mg/L) was added at the time of inoculation to accelerate establishment of reducing conditions and facilitate early growth.

Cultures were incubated at 37 °C for up to 5 days without shaking. Growth was monitored by visual inspection of turbidity and the formation of black iron sulfide (FeS) precipitate, which is characteristic of sulfate-reducing bacteria. Positive growth was also confirmed by the color change of the resazurin indicator from pink (oxidized) to colorless (reduced), verifying that anaerobic conditions were maintained throughout cultivation. At the end of the incubation period, the cultures had reached sufficient density to be used for preparation of dosing suspensions.

3.3 Preparation for Oral Gavage

E. coli K-12 cultures were harvested at mid-log phase ($OD_{600} \approx 0.4$–0.8), pelleted at 4 000 × g for 10 min, and washed twice with sterile Phosphate-buffered saline (PBS). The final suspension was adjusted to 5×10^8 Colony-forming units (CFU)/mL in PBS. Suspensions were kept on ice and administered within 2 h.

D. desulfuricans cultures were centrifuged at 4 000 × g for 10 min, washed twice with pre-reduced anaerobic PBS (PRAS; PBS sparged with N_2, supplemented with 0.05–0.1% L-cysteine and resazurin), and resuspended to 10^8 CFU/mL. Preparations were maintained under anoxic conditions until dosing.

3.4 Experimental Design

All procedures were approved by the Finnish National Board of Animal Experiments (license ESAVI/36853/2024) and performed in accordance with European Community guidelines. Prior to bacterial dosing, mice received antibiotics for 3 days (Ampicillin 1 g/L, Neomycin 1 g/L, Vancomycin 0.5 g/L, Metronidazole 1 g/L) followed by a 4-day washout period.

For oral gavage, mice were administered 200 µL bacterial suspension (1×10^8 CFU/mouse) three times weekly for four weeks using flexible gavage needles (AgnThos 5200). Fecal samples were collected one day after the washout period and one day before sacrifice. The dosing volume and administration procedures followed established guidelines for oral exposure studies (OECD, 2018)

After four weeks, mice were anesthetized with pentobarbital (90 mg/kg i.p., OrionPharma, diluted in saline) and sacrificed by transcardial perfusion with ice-cold PBS. Distal colons were dissected, flushed with PBS, and fixed in 4% paraformaldehyde (PFA in PBS) for 24 h at 4 °C. Colons were prepared as Swiss rolls, post-fixed in fresh PFA, dehydrated, and embedded in paraffin (Leica TP1020). Sections were cut at 10 µm thickness on a rotary microtome (Leica RM2235) and mounted on LABSOLUTE+ charged slides (TH. GEYER GMBH). Sections were stored at 4 °C until staining.

3.5 Immunohistochemistry

Antigen retrieval was performed on 10 µm paraffin sections, which had been dried overnight at 40 °C before staining. Slides were immersed in 10 mM sodium citrate buffer (pH 6.0; Sigma-Aldrich) containing 0.05% Tween-20 and heated in a microwave oven (600 W for 5 min, then 400 W for 6 min). Sections were treated with 0.3% H_2O_2 in Tris-buffered saline (TBS; 50 mM Tris, 150 mM NaCl, pH 7.6) for 30 min, rinsed three times in TBS containing 0.05% Tween-20 (TBS-T), and blocked in 1.5% normal goat serum (Vector Laboratories) for 30 min.

Primary antibodies were applied overnight at +4 °C in blocking solution. The phospho-S129 α-synuclein antibody was used at 1:500 dilution, and the CgA antibody at 1:100 dilution. After rinsing three times in TBS-T, sections were incubated with biotinylated secondary antibodies (Vector Laboratories) at 1:400 dilution for 1 h at room temperature, followed by incubation with the avidin–biotin complex (ABC; Vector Laboratories, PK-4000) for 30 min.

Visualization of α-synuclein staining was carried out with 3,3′-diaminobenzidine (DAB; Vector Laboratories, SK-4100) for 3 min. Alcian blue (1 g/100 mL in 3% acetic acid; Sigma-Aldrich) was applied for 30 min as a counterstain.

For double staining, phosphorylated α-synuclein was visualized first with DAB, after which sections were blocked with avidin/biotin reagent (Vector Laboratories, SP-2001) and incubated with CgA antibody (Antibodies.com, A307702) overnight at +4 °C. Detection used biotinylated secondary antibody (1:400), ABC reagent, and HistoGreen (Linaris, E109) for 2 min 40 s. Hematoxylin (1:10 in water; Sigma-Aldrich) was applied as counterstain.

Each incubation step was followed by three washes in TBS-T. After staining, slides were dehydrated through a graded ethanol series, cleared in xylene, and coverslipped with mounting medium.

Controls included positive control mouse forebrain tissue (for α-synuclein), heart tissue (negative for CgA), and isotype controls (Mouse IgM, Biolegend 401601; Rabbit IgG, Invitrogen 31735).

3.6 Imaging and Analysis

Slides were scanned at 20× magnification using a 3DHistech Pannoramic P250 scanner. Images were analyzed with QuPath v0.6.0. Regions of interest (ROIs) were annotated for α-synuclein aggregates, EECs, goblet cells, and immune cell infiltration. Object detection thresholds were standardized across all samples. For α-synuclein analysis, a pixel classifier was trained in QuPath to identify aggregates. Manual thresholding was used to maximize aggregate detection while minimizing signals from sources such as background, artifacts, and unspecific binding. To prevent multiple adjacent aggregates from being merged, a watershed-based script was applied. For CgA analysis, an additional classifier was trained to detect EECs. Each discrete CgA-positive signal was operationally defined as one EEC. All classifier outputs were manually inspected annotation by annotation, and corrections were made to remove misidentified objects. Final object sets were exported to Python (Jupyter Notebook) for statistical analysis.

Aggregate annotations were exported as per-sample CSVs. Goblet cells were manually annotated along the epithelial layer. Immune cell infiltration was recorded as discrete foci in mucosa or submucosa. For CgA–α-synuclein staining, EECs were annotated and nearest-neighbor distances to aggregates were calculated. Data handling and analysis were performed in Python 3 (Jupyter Notebook) using pandas, NumPy, SciPy, pathlib, and matplotlib.

3.7 Molecular Methods

DNA was extracted from fecal samples using the PureLink Microbiome DNA Purification Kit (Thermo Fisher Scientific, A29790) according to the manufacturer’s protocol. DNA concentration and purity were measured with a Nanodrop (Thermo Fisher Scientific). Between 0.01 and 0.1 g fecal matter was used per sample.

Detection of D. desulfuricans was performed by PCR targeting the 16S rRNA gene with primers described by Loubinoux et al. (2002):

- 27K-F: CTGCCTTTGATACTGCTTAG
- 27K-R: GGGCACCCTCTCGTTTCGGAGA

PCR products (396 bp expected size) were amplified in 20 µL reactions containing 1× Phusion Green HF buffer, 0.2 mM dNTP mix, 0.5 µM of each primer, 1 U Phusion High-Fidelity DNA polymerase, and 15–25 ng DNA. Thermal cycling: 98 °C 30 s; 30 cycles of 98 °C 10 s, 55–61 °C 10 s, 72 °C 20 s; final extension 72 °C 5 min; hold at 4 °C. PCR products were analyzed on 0.9–1.5% agarose gels containing ethidium bromide and visualized under UV light.

4 Results

4.1 Variation in fecal DNA concentrations between timepoints

Fecal samples were collected at two timepoints to evaluate how the amount of extracted DNA varied during the study and to identify the presence of D. Desulfuricans. The amounts of fecal matter used for most samples were close to 0.1 g, although smaller amounts were processed in cases where less material was available. (Figure 1) At Timepoint 1, immediately following the antibiotic treatment, DNA concentrations were generally low, ranging from 20 to 100 ng/µl in most samples (Figure 2). By contrast, at Timepoint 2, one month later, concentrations were consistently higher, frequently exceeding 150 ng/µl and in several cases surpassing 200 ng/µl (Figure 2). This pattern implies that microbial community recovery after the washout period was reflected in the higher DNA concentrations obtained from fecal material at the later timepoint. These measurements were used as a proxy for overall microbial biomass recovery following antibiotic treatment, since higher DNA concentrations generally indicate increased microbial load in fecal material.

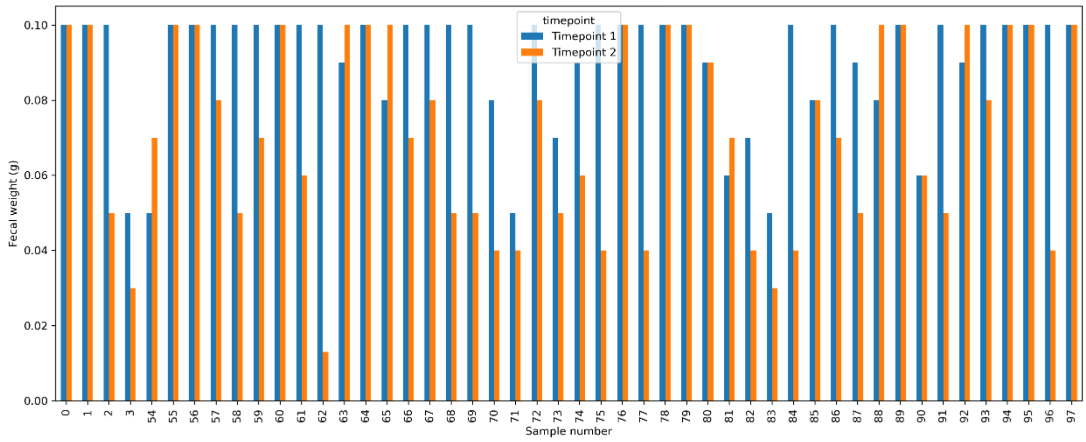

Figure 1. Fecal weights by sample at two timepoints: This bar plot compares fecal sample weights across two collection timepoints for all mice. Blue columns correspond with the first timepoint, while orange correspond with the second.

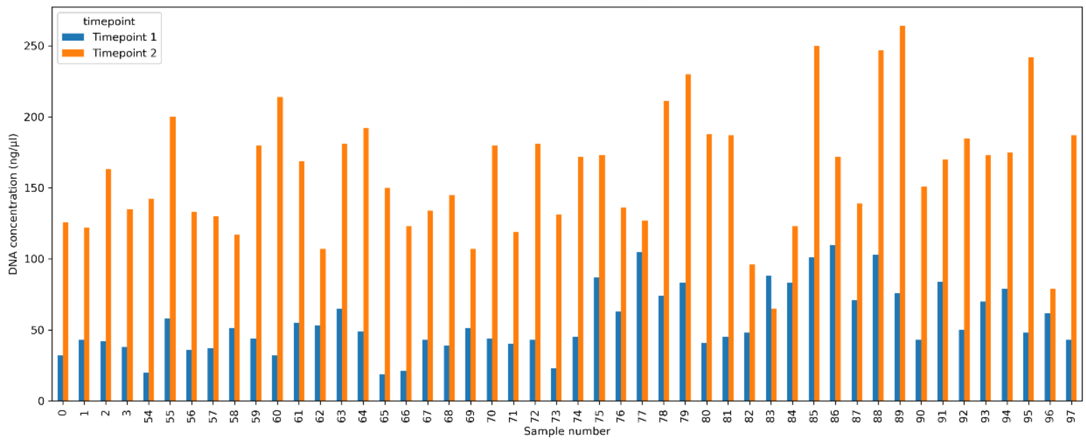

Figure 2. DNA concentrations by fecal sample at two timepoints. Bar plot shows DNA concentrations in ng/µl from fecal samples across the same two timepoints. Blue columns correspond with the first timepoint, while orange correspond with the second.

4.2 Non-specific amplifications limit detection of *D. Desulfuricans* via PCR

To quantify the presence of *D. desulfuricans* at different timepoints, PCR was performed on DNA extracted from fecal samples collected after the antibiotic washout period and one day prior to sacrifice. PCR products were evaluated using agarose gel electrophoresis and imaged. At the first timepoint, some samples showed multiple bands (Figure 3 A and B), suggesting unspecific primer binding, although faint bands of the expected size were present in most cases. The negative control showed no amplification, while the positive control produced a strong, single band. At the second timepoint (Figure 3 C and D), banding irregularities were more pronounced, with nearly all samples showing multiple non-specific products. Positive and negative controls again performed as expected.

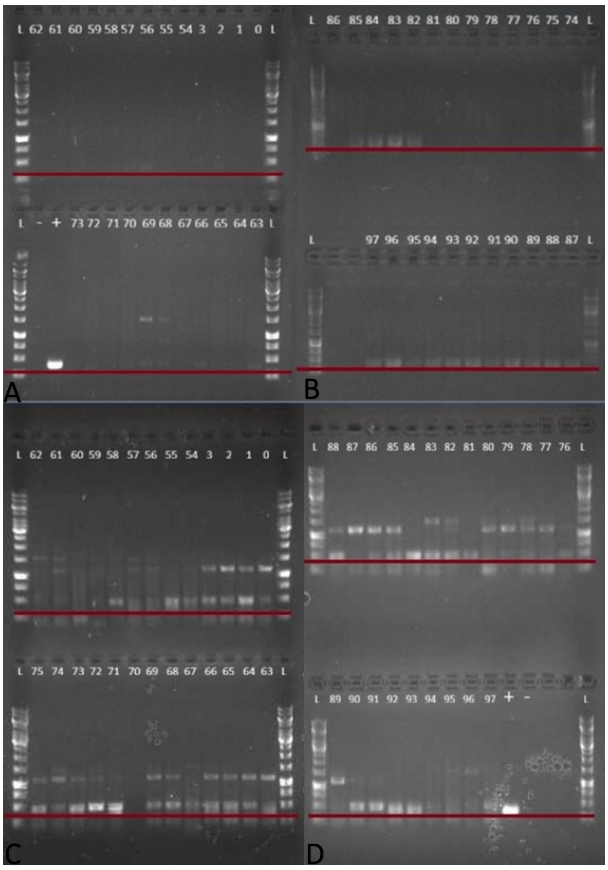

Figure 3. PCR amplification of mouse fecal DNA samples at two timepoint. A: Samples 0–73 from the first timepoint with positive and negative controls as well as DNA ladders on both sides. They are noted as +, -, and L respectively. B: Samples 74–97 from the same timepoint with corresponding DNA ladders. C: Samples 0–75 from the

first timepoint with corresponding DNA ladders. D: Samples 76–97 from the same timepoint with positive and negative controls as well as DNA ladders on both sides. A bright red line was added to each run gel set to approximately annotate correct band location, 400 bp.

To clarify these results, PCR validation was carried out using plasmid DNA from *E. coli MC4100, E. coli OP50, D. desulfuricans, D. piger, D. fairfidensis, D. vulgaris*, and a negative control (Figure 4). This analysis confirmed that the primers produced non-specific binding across several species, strongly suggesting that the earlier PCR results were confounded by primer non-specificity and thus not reliable indicators of *D. desulfuricans* abundance.

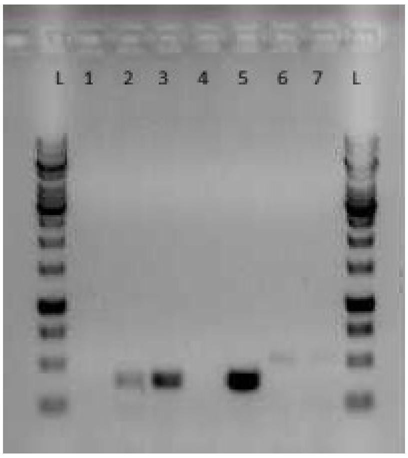

Figure 4. PCR primer validation using bacterial reference strains. From the left, following the DNA ladder: lane 1, negative control; lane 2, *D. vulgaris*; lane 3, *D. fairfieldensis*; lane 4, *D. piger*; lane 5, *D. desulfuricans*; lane 6, *E. coli OP50*; lane 7, *E. coli MC4100*.

Distinct amplicons were obtained in all strains except *D. piger* and the negative control, confirming primer non-specificity across multiple species. PCR was employed to specifically detect *D. desulfuricans* in the fecal samples, with the rationale that successful colonization would be evident as a band of expected size. However, primer non-specificity across several bacterial species prevented reliable interpretation of these results.

4.3 Validation of antibodies and staining protocols showed consistent results

Prior to staining, primary antibodies were validated on control samples, which showed no irregularities. Colon samples from a subset of animals were then processed through paraffin embedding, sectioning, and heat fixation before IHC. Two staining protocols were applied: DAB staining for pS129 α-synuclein with alcian blue co-staining. Double staining for α-synuclein and CgA, counterstained with hematoxylin.

4.4 Stained colon tissues show α-Synuclein aggregates, CgA signals, and some tissue deficits.

Both sets of stainings seemed successful upon inspection and antibody validation. Visual inspection revealed partial tissue damage in most samples, limiting the ability to consistently analyze identical regions. To account for this, two ROIs were manually annotated for each sample, defined as a comparable length starting from the center point of the Swiss-rolled colon section.

4.5 No significant group differences in pathological readouts

α-Synuclein–positive aggregates were quantified on a per-sample basis to avoid biases from unequal group sizes. Aggregate counts did not differ significantly between groups (Kruskal–Wallis test, $n = 35$, $p = 0.115$). (Figures 5 and 6). Aggregates were quantified to determine whether colonization with DSV strains was associated with increased α-synuclein pathology in the colon.

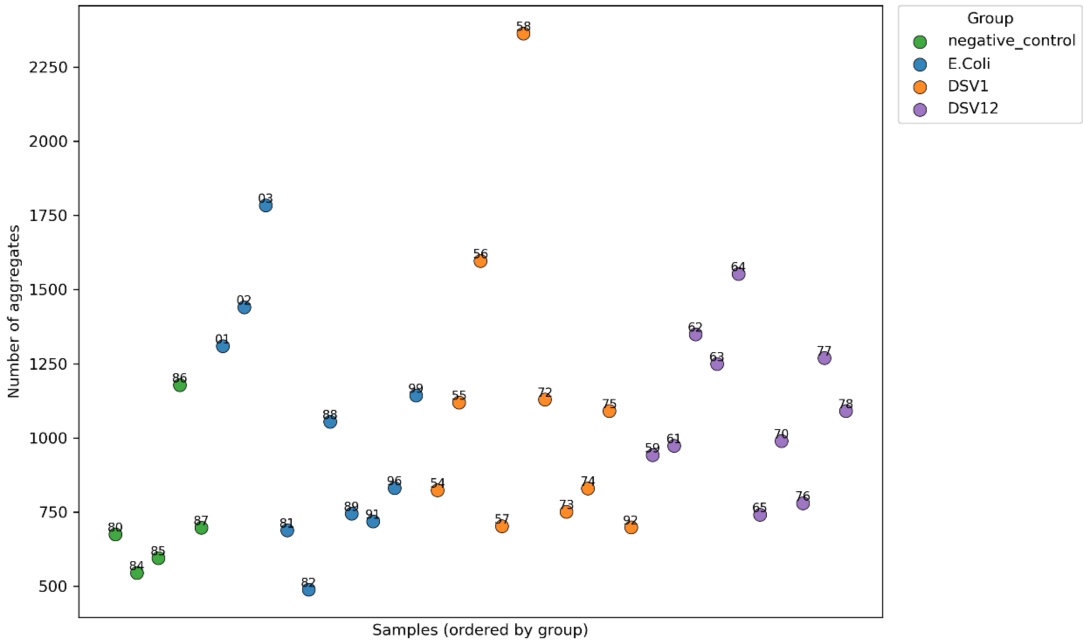

Figure 5. Scatter plot of the number of α-synuclein aggregates per sample, grouped by treatment condition. Each point represents one sample, color-coded by group. Green corresponds to the negative control group, Blue to *E. coli*, orange to DSV1 and purple to DSV12.

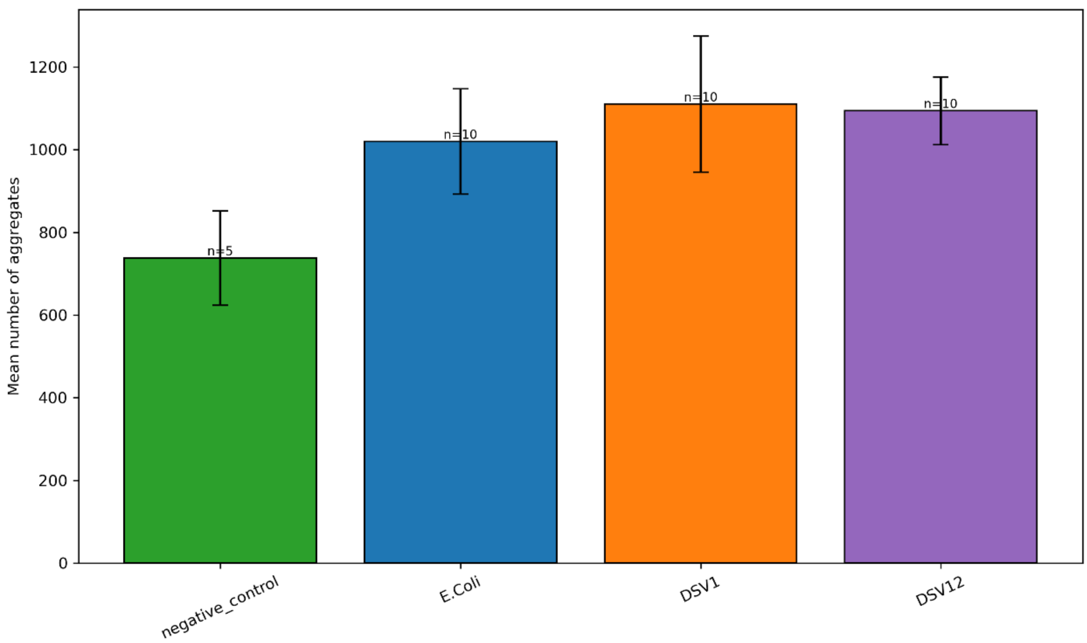

Figure 6. Bar plot of the mean number of α-synuclein aggregates per group with error bars noting the standard error of the mean (SEM). Sample sizes are indicated above each bar.

Immune cell infiltration counts per sample were low and tightly clustered (Table 1.) No statistically significant differences were found among groups (Kruskal–Wallis test, n = 35, p = 0.68). Crypt symmetry scores, on a scale from 0 to 1, where 1 is perfect symmetry, also showed minimal variance. No group showed a significantly different symmetry score (one-way ANOVA, n = 35, p = 0.75). Immune cell infiltration amounts and crypt symmetry were included as readouts of epithelial barrier integrity, since dysbiosis-associated inflammation is known to affect mucus production and epithelial symmetry (Pelaseyed et al., 2014b).

Table 1. Amounts of immune cell infiltrations and crypt symmetry scores divided by group.

Sample group	Amount of immune cell infiltrations (counts/sample, mean ± SEM)	Crypt symmetry scores (0–1, mean ± SEM)
Negative control	2.1 ± 0.5	0.95 ± 0.03
DSV1	2.2 ± 0.7	0.96 ± 0.02
DSV12	2.3 ± 0.6	0.95 ± 0.03
E. Coli	2.4 ± 0.6	0.94 ± 0.04

To assess spatial relationships, each EEC was assigned the distance to its nearest α-synuclein aggregate. Approximately 5% of EECs were located within 10 µm of an aggregate, while the majority lay beyond 20 µm, with reference anchors at 20 µm and 50 µm (Figure 7). The distance distributions are strongly right-skewed, with the highest density in the 0–10 µm and 10–20 µm bins and progressively fewer EECs at larger distances, yielding a long tail extending beyond 400 µm. The curves for all four groups overlap closely, indicating no clear group-wise shift in proximity. These distributions did not reveal significant group differences in proximity when summarized per sample (Kruskal–Wallis test, n = 35, p = 0.8). Distances between EECs and aggregates were measured to test the hypothesis that EECs may act as initiation sites of α-synuclein pathology, given their proposed role in gut–brain axis transmission.

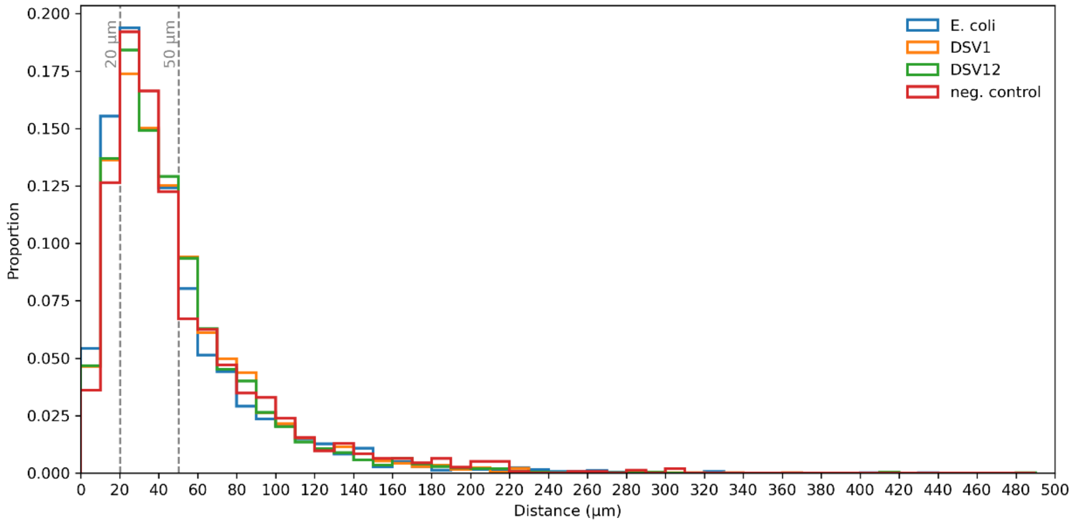

Figure 7. Normalized histograms showing the distribution of distances between each EEC and its closest α-synuclein aggregate. Plotted separately for each group: Vertical dashed lines at 20 µm and 50 µm serve as reference anchors.

Finally, EEC counts were quantified for each sample (Figure 8). Comparisons of EEC counts across groups did not reveal consistent or statistically significant differences (Kruskal–Wallis test, $n = 35$, $p = 0.54$).

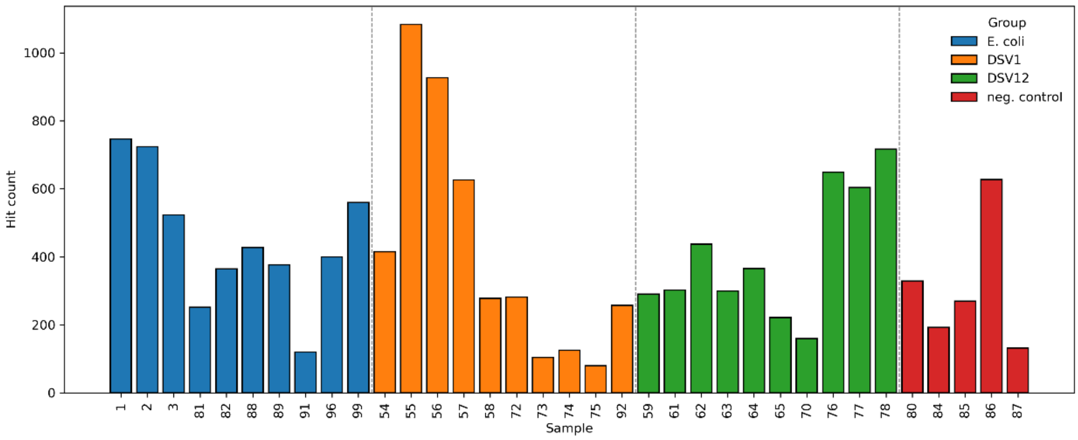

Figure 8. Bar plot showing the number of detected CgA–positive cells across all samples, grouped by treatment condition.

5 Discussion

The microbial component of this study relied on primers designed by Loubinoux et al. (2002) for the detection of DSV species in human fecal samples. While those primers were originally reported as highly specific, the present validation experiments indicated that they amplified products in *D. vulgaris, D. fairfieldensis*, and even Escherichia coli strains. This outcome suggested that the primers targeted conserved motifs within the 16S rRNA gene, a limitation that has been well documented for many “species-specific” primers (Klindworth et al., 2013). Off-target amplification can also result from intragenomic heterogeneity among 16S rRNA operons, as shown by Acinas et al. (2004), further complicating interpretation of PCR results. The weaker PCR bands observed in samples collected directly after antibiotic treatment paralleled the reduced DNA concentrations at this timepoint, consistent with reports that antibiotic exposure reduces microbial abundance and diversity in the gut (Modi et al., 2014). Together, these results demonstrated that the primer set was not suitable for accurate quantification of D. desulfuricans and highlight the need for updated primer design using expanded databases such as SILVA or RDP (Quast et al., 2013). Future studies would benefit from quantitative PCR with probe-based assays or metagenomic approaches, which can provide greater taxonomic resolution and avoid the interpretive uncertainties encountered here (Knight et al., 2018).

Both sets of IHC stainings produced clear and interpretable signals, with expected labeling of phosphorylated α-synuclein pS129 and CgA in positive control tissues. This confirmed that the antibodies recognized their intended targets and that the staining procedures were technically successful, consistent with earlier validations of these markers in neural and gastrointestinal tissues (Hilton et al., 2014). The successful detection of pS129 aggregates is particularly important, as this phosphorylated form is widely accepted as a pathological signature of α-synuclein aggregation in both human and experimental models (Anderson et al., 2006). Similarly, the reliable identification of CgA-positive EECs confirmed that the staining protocol could capture relevant epithelial subpopulations implicated in gut–brain signaling.

While variability in staining intensity was observed across samples, the overall ability to detect α-synuclein aggregates and CgA-positive cells demonstrated that the chromogenic approach was robust for systematic tissue-level analysis. Chromogenic IHC is frequently favored for high-throughput studies and long-term slide storage, and despite lower sensitivity compared to multiplex fluorescence approaches, it has been shown to provide reproducible results in gut and brain tissue alike (Shi et al., 2023). This supports its use here as a practical balance between technical feasibility and biological insight.

The IHC analyses did not reveal significant differences between treatment groups in terms of α-synuclein aggregates, EEC–aggregate proximity, EEC abundance, immune infiltration, or crypt symmetry. These findings suggested that if microbial colonization induced pathology, such effects were either too subtle to be detected with the chosen readouts or not yet established at the four-week endpoint. Previous animal studies have also reported heterogeneity in intestinal α-synuclein pathology, with patchy and inconsistent distribution across mucosal regions (Challis et al., 2020). Similarly, human biopsy studies demonstrate that α-synuclein deposition in the gastrointestinal tract is irregular and not always associated with specific epithelial or neuroendocrine cell types (Beach et al., 2021). The absence of preferential localization near EECs in this study aligns with those observations and supports the idea that if EECs contribute to pathology, such interactions may occur rarely or under specific inflammatory conditions not reproduced here.

The lack of group-wise differences in immune cell infiltration or crypt symmetry also pointed to the resilience of colonic architecture under the study conditions. Previous work has shown that goblet cell depletion and crypt symmetry disruption can be sensitive indicators of mucosal stress in models of colitis or microbiota-induced inflammation (Pelaseyed et al., 2014a). Their preservation here therefore suggests that DSV colonization did not reach a threshold sufficient to disrupt barrier function within the examined timeframe. Visual inspection of infiltrates confirmed their presence but not their magnitude or cellular identity, leaving open the possibility of subtle immune responses that were not captured by the chosen readouts. Complementary analyses, such as cytokine profiling, tight-junction staining, or multiplex immunophenotyping, have been shown to reveal subclinical alterations in similar contexts (Houser & Tansey, 2017; Yang et al., 2021) and should be considered in future studies.

Overall, the IHC results indicated that the applied methods successfully detected the intended molecular targets and tissue structures, but they did not reveal strong group-dependent differences. This outcome is consistent with the broader literature showing that intestinal α-synuclein pathology is often heterogeneous, sporadic, and influenced by multiple host and environmental factors on a longer time period that what was used here (Kim et al., 2019; Sampson et al., 2016). The findings here therefore add to the evidence that microbial effects on α-synuclein aggregation in mammals may be modest, require longer exposure, or depend on additional sensitizing conditions beyond wildtype genetic background.

Evidence obtained in C. elegans models should be interpreted cautiously when extrapolated to mammals. Even when a more complex microbiome is introduced, the host–microbe ecosystem remains far less diverse and spatially structured than in mammals. As a result, strain-level microbial effects on host phenotypes can appear large in C. elegans because competitive ecological buffering and niche redundancy are limited (Gerbaba et al., 2017).

By contrast, the murine gut microbiota exhibits markedly greater taxonomic and functional complexity, mucosal compartmentalization, and immune surveillance, all of which contribute to colonization resistance, i.e., community-level mechanisms that suppress invasion or overgrowth of individual taxa. This ecological buffering reduces the host-level impact of introducing a single exogenous strain, unless the community has been destabilized or the strain confers a strong fitness advantage. These principles are well established in mouse studies of colonization resistance and microbial ecology (Buffie & Pamer, 2013).

Translating further to humans introduces additional divergence. Although murine and human gut microbiomes share broad functional capacities, they differ substantially in composition and relative abundances, and human communities are typically more diverse and individualized. These differences limit the one-to-one transfer of single-taxon effects observed in rodents (Nguyen et al., 2015). Consequently, microbial manipulations that robustly modulate Parkinson's-related readouts in gnotobiotic or antibiotic-conditioned mice can attenuate or vary widely across human hosts (Sampson et al., 2016).

Thus, while invertebrate models such as C. elegans can demonstrate striking effects of individual strains on α-synuclein aggregation (Huynh et al., 2023; Mohammadi et al., 2025), the murine gut represents a more complex and resilient microbial ecosystem, in which colonization resistance and functional redundancy attenuate the impact of any one taxon (Buffie & Pamer, 2013; Kamada et al., 2013). In humans, this complexity is further amplified by interindividual variability, lifestyle, and genetic background, making it unlikely that a single microbial species alone drives pathology (Falony et al., 2016). These considerations suggest that future work should adopt a community-level approach, investigating how consortia of microbes and their metabolic interactions shape host vulnerability to α-synuclein misfolding and neuroinflammation (Sharon et al., 2016). Moreover, it must be acknowledged that PD develops over decades in humans, and short-term colonization models may not capture the protracted timescales required for pathology to emerge (Kalia & Lang, 2015; Braak & Del Tredici, 2017). Thus, the absence of substantial group-specific differences in the present study does not preclude microbial contributions to disease.

Furthermore, the exclusive use of wildtype male mice imposes several constraints on interpretation. Unlike transgenic or knockout models carrying mutations in genes such as SNCA, LRRK2, or GBA1, wildtype animals lack known genetic vulnerabilities that predispose to α-synuclein misfolding or dopaminergic neurodegeneration. As described by He et al. (2024), the wildtype mouse model is therefore best regarded as a reference for investigating prodromal phases of Parkinson's disease, since it does not spontaneously recapitulate the core pathological features of the disorder. This design increases internal consistency but means that microbial perturbations must overcome a higher threshold to elicit pathology, and subtle effects may remain below detection.

oyd

In addition, sex differences further limit the generalizability of the findings. Male and female mice, as well as humans differ in gut microbiota composition, diversity, and immune responsiveness (McGee et al., 2021; Kim et al., 2020). Hormonal influences on mucosal immunity and barrier function also shape host–microbe interactions in sex-specific ways (Shobeiri et al., 2022). By restricting the study to males, potential sex-dependent effects of microbial colonization on inflammation or α-synuclein pathology could not be captured. Since PD affects both men and women, with differences in incidence and progression, future studies should incorporate both sexes alongside genetically predisposed models to more fully reflect the multifactorial host context in which gut microbial contributions to PD unfold.

The absence of significant group-specific differences in α-synuclein aggregates, EEC proximity, or histological markers should also be interpreted in light of the study design. The modest sample size limited statistical power, increasing the likelihood that subtle effects were not detected. In addition, the short four-week timeframe contrasts with the decades-long progression of PD in humans, making it possible that relevant pathology had not yet emerged within this period. Future studies with longer colonization, repeated sampling, and larger cohorts would help determine whether the absence of observed differences reflects genuine biological resilience or simply methodological constraints. Incorporating community-level manipulations, such as defined microbial consortia rather than single-strain colonization, could further clarify whether microbial effects on α-synuclein aggregation require more complex or prolonged ecological interactions.

6 conclusions

This study evaluated whether colonization with *D. desulfuricans* influences colonic pathology in wild-type mice, focusing on α-synuclein aggregation, EECs, goblet cells, and immune cell infiltration. The analyses did not reveal significant differences between experimental and control groups, and only limited spatial association was observed between α-synuclein aggregates and EECs. These findings indicate that short-term colonization with *D. desulfuricans* is not sufficient to induce PD-like pathology in the mouse colon. The results therefore provide an important baseline for refining microbial models of PD and show the need for future work to incorporate longer experimental timeframes, genetically susceptible models, and community-level microbial interactions to clarify the contribution of gut microbiota to PD pathogenesis.

References:

Acinas, S.G., Marcelino, L.A., Klepac-Ceraj, V., and Polz, M.F., 2004. Divergence and Redundancy of 16S rRNA Sequences in Genomes with Multiple rrn Operons. *Journal of Bacteriology*, 186 (9), 2629–2635.

Andersen KB, Krishnamurthy A, Just MK, Van Den Berge N, Skjærbæk C, Horsager J, Knudsen K, Vogel JW, Toledo JB, Attems J, Polvikoski T, Saito Y, Murayama S, Borghammer P. Sympathetic and parasympathetic subtypes of body-first Lewy body disease observed in postmortem tissue from prediagnostic individuals. Nat Neurosci. 2025 May;28(5):925-936. doi: 10.1038/s41593-025-01910-9. Epub 2025 Mar 13. PMID: 40082617; PMCID: PMC12081295.

Beach TG, Adler CH, Sue LI, Shill HA, Driver-Dunckley E, Mehta SH, Intorcia AJ, Glass MJ, Walker JE, Arce R, Nelson CM, Serrano GE. Vagus Nerve and Stomach Synucleinopathy in Parkinson's Disease, Incidental Lewy Body Disease, and Normal Elderly Subjects: Evidence Against the "Body-First" Hypothesis. J Parkinsons Dis. 2021;11(4):1833-1843. doi: 10.3233/JPD-212733. PMID: 34151862; PMCID: PMC10082635.

Beach TG, Adler CH, Sue LI, Vedders L, Lue L, White Iii CL, Akiyama H, Caviness JN, Shill HA, Sabbagh MN, Walker DG; Arizona Parkinson's Disease Consortium. Multi-organ distribution of phosphorylated alpha-synuclein histopathology in subjects with Lewy body disorders. Acta Neuropathol. 2010 Jun;119(6):689-702. doi: 10.1007/s00401-010-0664-3. Epub 2010 Mar 21. PMID: 20306269; PMCID: PMC2866090.

Bedarf JR, Hildebrand F, Coelho LP, Sunagawa S, Bahram M, Goeser F, Bork P, Wüllner U. Functional implications of microbial and viral gut metagenome changes in early stage L-DOPA-naïve Parkinson's disease patients. Genome Med. 2017 Apr 28;9(1):39. doi: 10.1186/s13073-017-0428-y. Erratum in: Genome Med. 2017 Jun 29;9(1):61. doi: 10.1186/s13073-017-0451-z. PMID: 28449715; PMCID: PMC5408370.

Bohórquez DV, Shahid RA, Erdmann A, Kreger AM, Wang Y, Calakos N, Wang F, Liddle RA. Neuroepithelial circuit formed by innervation of sensory enteroendocrine cells. J

Clin Invest. 2015 Feb;125(2):782-6. doi: 10.1172/JCI78361. Epub 2015 Jan 2. PMID: 25555217; PMCID: PMC4319442. Borghammer P, Van Den Berge N. Brain-First versus Gut-First Parkinson's Disease: A Hypothesis. J Parkinsons Dis. 2019;9(s2):S281-S295. doi: 10.3233/JPD-191721. PMID: 31498132; PMCID: PMC6839496.

Borghammer P, Van Den Berge N. Brain-First versus Gut-First Parkinson's Disease: A Hypothesis. J Parkinsons Dis. 2019;9(s2):S281-S295. doi: 10.3233/JPD-191721. PMID: 31498132; PMCID: PMC6839496.

Braak H, Del Tredici K. Neuropathological Staging of Brain Pathology in Sporadic Parkinson's disease: Separating the Wheat from the Chaff. J Parkinsons Dis. 2017;7(s1):S71-S85. doi: 10.3233/JPD-179001. PMID: 28282810; PMCID: PMC5345633.

Braak H, Del Tredici K, Rüb U, de Vos RA, Jansen Steur EN, Braak E. Staging of brain pathology related to sporadic Parkinson's disease. Neurobiol Aging. 2003 Mar-Apr;24(2):197-211. doi: 10.1016/s0197-4580(02)00065-9. PMID: 12498954.

Buffie CG, Pamer EG. Microbiota-mediated colonization resistance against intestinal pathogens. Nat Rev Immunol. 2013 Nov;13(11):790-801. doi: 10.1038/nri3535. Epub 2013 Oct 7. PMID: 24096337; PMCID: PMC4194195.

Burke RE, Dauer WT, Vonsattel JP. A critical evaluation of the Braak staging scheme for Parkinson's disease. Ann Neurol. 2008 Nov;64(5):485-91. doi: 10.1002/ana.21541. PMID: 19067353; PMCID: PMC2605160.

Carbonero, F., Benefiel, A.C., Alizadeh-Ghamsari, A.H., and Gaskins, H.R., 2012. Microbial pathways in colonic sulfur metabolism and links with health and disease. *Frontiers in Physiology*, 3.

Challis C, Hori A, Sampson TR, Yoo BB, Challis RC, Hamilton AM, Mazmanian SK, Volpicelli-Daley LA, Gradinaru V. Gut-seeded α-synuclein fibrils promote gut dysfunction and brain pathology specifically in aged mice. Nat Neurosci. 2020 Mar;23(3):327-336. doi: 10.1038/s41593-020-0589-7. Epub 2020 Feb 17. PMID: 32066981; PMCID: PMC7065967.

Chandra, R., et al. (2017). *The role of the gut–brain axis in Parkinson's disease: Insights from enteroendocrine cell biology*. Journal of Neurochemistry, 143(6), 611–619.

Gao, X., Chen, H., Schwarzschild, M.A., and Ascherio, A., 2011. Use of ibuprofen and risk of Parkinson disease. *Neurology*, 76 (10), 863–869.

Gerbaba TK, Green-Harrison L, Buret AG. Modeling Host-Microbiome Interactions in *Caenorhabditis elegans*. J Nematol. 2017 Dec;49(4):348-356. PMID: 29353922; PMCID: PMC5770281.

Gerhardt, S. and Mohajeri, M.H., 2018. Changes of Colonic Bacterial Composition in Parkinson's Disease and Other Neurodegenerative Diseases. *Nutrients*, 10 (6), 708.

Hawkes CH, Del Tredici K, Braak H. Parkinson's disease: a dual-hit hypothesis. Neuropathol Appl Neurobiol. 2007 Dec;33(6):599-614. doi: 10.1111/j.1365-2990.2007.00874.x. Epub 2007 Oct 24. PMID: 17961138; PMCID: PMC7194308.

He, S. Ru, Q. Chen, L. Xu, G. Wu, Y. Advances in animal models of Parkinson's disease, Brain Research Bulletin, Volume 215, 2024, 111024, ISSN 0361-9230, https://doi.org/10.1016/j.brainresbull.2024.111024.

Hilton, D. A., et al. (2014). *Accumulation of α-synuclein in the bowel of patients in the pre-clinical phase of Parkinson's disease*. Acta Neuropathologica, 127(2), 235–241.

Houser, M.C. and Tansey, M.G., 2017. The gut-brain axis: is intestinal inflammation a silent driver of Parkinson's disease pathogenesis?. *npj Parkinson's Disease*, 3 (1).

Jenner P, Morris HR, Robbins TW, Goedert M, Hardy J, Ben-Shlomo Y, Bolam P, Burn D, Hindle JV, Brooks D. Parkinson's disease--the debate on the clinical phenomenology, aetiology, pathology and pathogenesis. J Parkinsons Dis. 2013;3(1):1-11. doi: 10.3233/JPD-130175. PMID: 23938306; PMCID: PMC4078250.

Johnson, A. M., Ou, Z. A., Gordon, R., & Saminathan, H. (2022). Environmental neurotoxicants and inflammasome activation in Parkinson's disease – a focus on the gut–brain axis. *International Journal of Biochemistry & Cell Biology*, 142, 106113.

Johnson, M.E., Stecher, B., Labrie, V., Brundin, L., and Brundin, P., 2019. Triggers, Facilitators, and Aggravators: Redefining Parkinson's Disease Pathogenesis. *Trends in Neurosciences*, 42 (1), 4–13.

Huynh, V. A., Takala, T. M., Murros, K. E., Diwedi, B., & Saris, P. E. J. (2023). *Desulfovibrio* bacteria enhance alpha-synuclein aggregation in a *Caenorhabditis elegans* model of Parkinson's disease. *Frontiers in Cellular and Infection Microbiology*, 13, 1181315.

Kalia LV, Lang AE. Parkinson's disease. Lancet. 2015 Aug 29;386(9996):896-912. doi: 10.1016/S0140-6736(14)61393-3. Epub 2015 Apr 19. PMID: 25904081.

Keshavarzian A, Green SJ, Engen PA, Voigt RM, Naqib A, Forsyth CB, Mutlu E, Shannon KM. Colonic bacterial composition in Parkinson's disease. Mov Disord. 2015 Sep;30(10):1351-60. doi: 10.1002/mds.26307. Epub 2015 Jul 16. PMID: 26179554.

Kim, S., Kwon, S.-H., Kam, T.-I., Panicker, N., Karuppagounder, S. S., Lee, S., Lee, J. H., Kim, W. R., Kook, M., Foss, C. A., Shen, C., Lee, H., Kulkarni, S., Pasricha, P. J., Lee, G., Pomper, M. G., Dawson, V. L., Dawson, T. M., & Ko, H. S. (2019). Transneuronal propagation of pathologic α-synuclein from the gut to the brain models Parkinson's disease. *Neuron*, 103(4), 627–641.e7. DOI: 10.1016/j.neuron.2019.05.035.

Kim YS, Unno T, Kim BY, Park MS. Sex Differences in Gut Microbiota. World J Mens Health. 2020 Jan;38(1):48-60. doi: 10.5534/wjmh.190009. Epub 2019 Mar 25. PMID: 30929328; PMCID: PMC6920072.

Klindworth, A., Pruesse, E., Schweer, T., Peplies, J., Quast, C., Horn, M., and Glöckner, F.O., 2013. Evaluation of general 16S ribosomal RNA gene PCR primers for classical and next-generation sequencing-based diversity studies. *Nucleic Acids Research*, 41 (1), e1–e1.

Knight R, Vrbanac A, Taylor BC, Aksenov A, Callewaert C, Debelius J, Gonzalez A, Kosciolek T, McCall LI, McDonald D, Melnik AV, Morton JT, Navas J, Quinn RA, Sanders JG, Swafford AD, Thompson LR, Tripathi A, Xu ZZ, Zaneveld JR, Zhu Q, Caporaso JG, Dorrestein PC. Best practices for analysing microbiomes. Nat Rev Microbiol. 2018 Jul;16(7):410-422. doi: 10.1038/s41579-018-0029-9. PMID: 29795328.

Kouli, A., Torsney, K.M., and Kuan, W.-L., 2018. Parkinson's Disease: Etiology, Neuropathology and Pathogenesis. *In*:.3–26. DOI: https://doi.org/10.15586/codonpublications.parkinsonsdisease.2018.ch1

Loubinoux, J., Bronowicki, J. P., Pereira, I. A. C., Mougenel, J. L., & Le Faou, A. E. (2002). Sulfate-reducing bacteria in human feces and their association with inflammatory bowel diseases. *FEMS Microbiology Ecology*, 40, 107–112. https://doi.org/10.1111/j.1574-6941.2002.tb00942.x.

Lubomski M, Xu X, Holmes AJ, Muller S, Yang JYH, Davis RL, Sue CM. The Gut Microbiome in Parkinson's Disease: A Longitudinal Study of the Impacts on Disease Progression and the Use of Device-Assisted Therapies. Front Aging Neurosci. 2022 May 17;14:875261. doi: 10.3389/fnagi.2022.875261. PMID: 35656540; PMCID: PMC9152137.

Luk, K. C., Kehm, V., Carroll, J., Zhang, B., O'Brien, P., Trojanowski, J. Q., & Lee, V. M. 2012. Pathological α-synuclein transmission initiates Parkinson-like neurodegeneration in non-transgenic mice. *Science*, 338(6109), 949–953. DOI: https://www.science.org/doi/10.1126/science.1227157.

Modi, S.R., Collins, J.J., and Relman, D.A., 2014. Antibiotics and the gut microbiota. *Journal of Clinical Investigation*, 124 (10), 4212–4218.

Mohammadi, K., Zhang, D., & Saris, P. E. J. (2025). Strain-specific effects of Desulfovibrio on neurodegeneration and oxidative stress in a Caenorhabditis elegans PD model. *NPJ Parkinson's disease*, *11*(1), Article 236. https://doi.org/10.1038/s41531-025-01102-z

Murros, K.E., Huynh, V.A., Takala, T.M., and Saris, P.E.J., 2021. Desulfovibrio Bacteria Are Associated With Parkinson's Disease. *Frontiers in Cellular and Infection Microbiology*, 11.

Nguyen TL, Vieira-Silva S, Liston A, Raes J. How informative is the mouse for human gut microbiota research? Dis Model Mech. 2015 Jan;8(1):1-16. doi: 10.1242/dmm.017400. PMID: 25561744; PMCID: PMC4283646.

Nuzum, N.D., Loughman, A., Szymlek-Gay, E.A., Teo, W.-P., Hendy, A.M., and Macpherson, H., 2022. To the Gut Microbiome and Beyond: The Brain-First or Body-First Hypothesis in Parkinson's Disease. *Frontiers in Microbiology*, 13.

OECD. (2018). *OECD Guidance Document on Acute Oral Toxicity Testing*. Organisation for Economic Co-operation and Development, Paris.

Pelaseyed, T., Bergström, J.H., Gustafsson, J.K., Ermund, A., Birchenough, G.M.H., Schütte, A., Van Der Post, S., Svensson, F., Rodríguez-Piñeiro, A.M., Nyström, E.E.L., Wising, C., Johansson, M.E.V., and Hansson, G.C., 2014. The mucus and mucins of the goblet cells and enterocytes provide the first defense line of the gastrointestinal tract and interact with the immune system. *Immunological Reviews*, 260 (1), 8–20.

Pelaseyed, T., et al. 2014. The mucus and mucins of the goblet cells and enterocytes provide the first defense line of the gastrointestinal tract and interact with the immune system. *Nature Reviews Gastroenterology & Hepatology*, 11(12), 717–726.

Quast, C., Pruesse, E., Yilmaz, P., Gerken, J., Schweer, T., Yarza, P., Peplies, J., and Glöckner, F.O., 2012. The SILVA ribosomal RNA gene database project: improved data processing and web-based tools. *Nucleic Acids Research*, 41 (D1), D590–D596.

Rey, N. L., Steiner, J. A., Maroof, N., Luk, K. C., Madaj, Z., Trojanowski, J. Q., & Brundin, P. (2013). Widespread transneuronal propagation of α-synucleinopathy triggered in olfactory bulb mimics prodromal Parkinson's disease. *Journal of Experimental Medicine*, 210(5), 2575–2583. DOI: [10.1084/jem.20160368](10.1084/jem.20160368)

Romano, S., Savva, G.M., Bedarf, J.R., Charles, I.G., Hildebrand, F., and Narbad, A., 2021. Meta-analysis of the Parkinson's disease gut microbiome suggests alterations linked to intestinal inflammation. *npj Parkinson's Disease*, 7 (1).

Sampson, T.R., Debelius, J.W., Thron, T., Janssen, S., Shastri, G.G., Ilhan, Z.E., Challis, C., Schretter, C.E., Rocha, S., Gradinaru, V., Chesselet, M.-F., Keshavarzian, A., Shannon, K.M., Krajmalnik-Brown, R., Wittung-Stafshede, P., Knight, R., and Mazmanian, S.K., 2016. Gut Microbiota Regulate Motor Deficits and Neuroinflammation in a Model of Parkinson’s Disease. *Cell*, 167 (6), 1469–1480.e12.

Shannon KM, Keshavarzian A, Dodiya HB, Jakate S, Kordower JH. Is alpha-synuclein in the colon a biomarker for premotor Parkinson's disease? Evidence from 3 cases. Mov Disord. 2012 May;27(6):716-9. doi: 10.1002/mds.25020. Epub 2012 May 1. PMID: 22550057.

Shi J, Wang Y, Chen D, Xu X, Li W, Li K, He J, Su W, Luo Q. The alteration of intestinal mucosal α-synuclein expression and mucosal microbiota in Parkinson's disease. Appl Microbiol Biotechnol. 2023 Mar;107(5-6):1917-1929. doi: 10.1007/s00253-023-12410-w. Epub 2023 Feb 16. PMID: 36795141; PMCID: PMC10006030.

Shobeiri, P., Kalantari, A., Teixeira, A.L., and Rezaei, N., 2022. Shedding light on biological sex differences and microbiota–gut–brain axis: a comprehensive review of its roles in neuropsychiatric disorders. *Biology of Sex Differences*, 13 (1).

Stiernagle, T. (2006). Maintenance of *C. elegans*. *WormBook*, ed. The C. elegans Research Community, WormBook. https://www.wormbook.org/chapters/www_strainmaintain/strainmaintain.html

Svensson, E., Horváth-Puhó, E., Thomsen, R. W., Djurhuus, J. C., Pedersen, L., Borghammer, P., & Sørensen, H. T. (2015). Vagotomy and subsequent risk of Parkinson’s disease. *Annals of Neurology*, 78(4), 522–529. DOI: **https://doi.org/10.1002/ana.24448**.

Tsutsumi Y. Pitfalls and Caveats in Applying Chromogenic Immunostaining to Histopathological Diagnosis. Cells. 2021 Jun 15;10(6):1501. doi: 10.3390/cells10061501. PMID: 34203756; PMCID: PMC8232789.

Yang H, Shao Y, Hu Y, Qian J, Wang P, Tian L, Ni Y, Li S, Al-Nusaif M, Liu C, Le W. Fecal microbiota from patients with Parkinson's disease intensifies inflammation and neurodegeneration in A53T mice. CNS Neurosci Ther. 2024 Aug;30(8):e70003. doi: 10.1111/cns.70003. PMID: 39161161; PMCID: PMC11333719.

Yang, S., Li, X., Wang, Y., & Liu, Y. 2021. Role of Goblet Cells in Intestinal Barrier and Mucosal Immunity. *Journal of Inflammation Research*, **14**, 3797–3810. DOI: 10.2147/JIR.S318327.

Zhang J, Shi M, Zhang Q, Chen Y, Yin X, Wang X, Zhang Y. Association between Constipation and the Risk of Parkinson's Disease among Participants in the UK Biobank. Neuroepidemiology. 2025;59(4):381-390. doi: 10.1159/000540955. Epub 2024 Aug 19. PMID: 39159603. DOI: 10.1159/000540955.